CrossMark

# Influence of Supporting Electrolytes on Electrochemical Treatability of Reactive Black 5 Using Dimensionally Stable Anode

Priya Saxena[1] · Jayesh Ruparelia[1]

**Abstract** Dye wastewaters contain significant amounts of toxic organic species and intense color. Electrochemical oxidation has a proven potential to degrade these bio-resistant pollutants. This paper presents the results of indirect electrochemical oxidation of Reactive Black 5 (RB 5) recalcitrant dye wastewater using NaCl, KBr and $Na_2SO_4$ as supporting electrolytes. The studies were performed in an undivided batch reactor using indigenously prepared Ti/$CoO_x$–$RuO_2$–$SnO_2$–$Sb_2O_5$ electrode classified as dimensionally stable anode (DSA). Characterization of the catalytic coating was performed using scanning electron microscopy (SEM), X-ray diffraction (XRD) and energy-dispersive X-ray (EDAX) analysis. Similar operating conditions like electrolyte concentration, pH, current density and electrolysis time were used for all studies. The progress of dye degradation was monitored by estimating reduction in chemical oxygen demand (COD), total organic carbon (TOC) and color. Other performance indicators like average current efficiency (ACE) and energy consumption (EC) were also analyzed. The rate of COD removal followed pseudo-first-order kinetics. The present investigation exhibited highest treatment effectiveness in the presence of chloride compared to bromide and sulfate as degradation was dependent on the generation of highly electroactive oxidative species.

**Keywords** Reactive Black 5 · Electrochemical · Supporting electrolytes · DSA · Characterization

✉ Priya Saxena
   priyasaxena2080@gmail.com

1  Department of Chemical Engineering, Institute of Technology, Nirma University, Ahmedabad, Gujarat, India

## Introduction

Textile dyeing processes typically generate effluents containing high concentrations of recalcitrant organic compounds and inorganic salts. These effluents are characterized by intense color, high COD and TOC with wide pH variation and present a potential source of non-aesthetic pollution, eutrophication, reduced gas solubility and diminished transparency to natural light, thereby hampering the natural process of photosynthesis [1–3]. Reactive azo dyes are of special interest due to their extensive use in dyeing processes. The fact that these dyes undergo a hydrolysis reaction with the fiber to a limited extent leads to the generation of highly concentrated toxic effluent exhibiting carcinogenic and mutagenic properties due to the presence of azo (–N=N–) species [4–8].

Conventional biological treatment is found to be unsuitable to treat dyehouse effluent due to its resistance to biodegradation [1]. In recent years, the electrochemical processes are gaining greater attention among diverse advanced oxidation processes due to their versatility, ease of operation, energy efficiency, and cost-effectiveness. In electrochemical oxidation, electron serves as the main reagent for redox reactions, called "clean reagent" without generating any secondary pollutant in the form of sludge [1, 3, 5, 9–11]. The efficacy and pollutant degradation pathway of electrochemical oxidation is strongly governed by the choice of electrode or anode material, current density and supporting electrolyte [12]. DSA® class of electrodes have gained popularity for wastewater treatment applications due to their high surface area, performance, stability in terms of excellent mechanical and chemical resistance even at high current density, cost and lifetime even in strongly acid media [7, 13, 14]. Dimensionally stable anodes (DSAs) represent a special class of active electrodes formed by

🐾 Springer

300

J. Inst. Eng. India Ser. A (June 2019) 100(2):299–310

mixing various metal oxides especially, containing $RuO_2$ or $IrO_2$, and depositing this mixture over pretreated inert substrate like Ti, SS, C and Si. Such mixing of metal oxides along with Sb–Sn doping results in formation of new stable compounds with high surface area, thereby significantly enhancing the catalytic activity as well as stability and service life of the anode. It has been reported that recalcitrant organic pollutants including dyes can be efficiently degraded by direct or indirect (mediated) electrochemical oxidation at these anodes. These anodes favor low chlorine evolution overpotential which is beneficial in generating electroactive chlorine oxidant species at the anode surface in effluents containing chlorides [15].

Sodium sulfate ($Na_2SO_4$), sodium chloride (NaCl), potassium chloride (KCl), sodium perchlorate ($NaClO_4$), sodium nitrate ($NaNO_3$) and sodium carbonate ($Na_2CO_3$) are commonly used supporting electrolytes [4, 13, 16, 17]. Addition of these supporting electrolytes to the reaction mixture enhances the solution conductivity, helps to reduce the resistance of system and also contributes to lower the energy cost of the process [1]. The use of different chloride-, sulfate-, bromide-, nitrate- and carbonate-based electrolytes has been reported for electrochemical degradation of various compounds like resorcinol [13], catechol [18], herbicide [9], dye and dyehouse effluents [4, 5, 8, 11, 16]. The generation of oxidative species from the supporting electrolyte can also contribute to pollutant degradation [12]. An electrochemical process typically involves anodic oxidation reaction and cathodic reduction reaction. Such redox reactions can lead to partial degradation or complete mineralization of organic pollutants [16]. Two mechanisms are proposed for electrochemical degradation of organic matter: (1) direct anodic oxidation where the pollutants are first adsorbed at the anode surface and destroyed by the anodic electron transfer reaction and (2) indirect oxidation in the liquid bulk which is mediated by the in situ electrogenerated active oxidants.

In the present work, an attempt was made to investigate the effect of supporting electrolytes like NaCl, KBr and $Na_2SO_4$ on electrooxidation performance of synthetic RB 5 dye wastewater using indigenously fabricated and characterized Ti/$CoO_x$–$RuO_2$–$SnO_2$–$Sb_2O_5$ electrode as DSA. Under similar electrolysis parameters, COD and TOC decay and color reduction was monitored for each electrolyte tested. Average current efficiency, energy consumption and kinetics based on COD removal rate were also examined.

## Materials

In the present work, a textile reactive azo dye Reactive Black 5 (RB 5, $\lambda_{max}$ = 597) was chosen as model pollutant. It was procured from a local source and used as received.
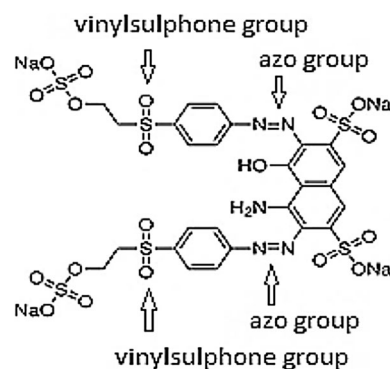


Fig. 1 C.I. Reactive Black 5

As shown in Fig. 1, it is one of the most commonly used recalcitrant dyestuffs in cotton dyeing contributing to concentrated dyeing effluents due to its high molecular weight and structural complexity [3, 6, 19]. It has been reported that the use of metals such as Ti/Pt, pure Pt, Ir, Pd, Ni, Co and Ag in indirect electrooxidation with active chlorine can yield rapid decomposition and color reduction in highly concentrated dye wastewaters [7]. In this study, a synthetic solution containing 1000 ppm RB 5 was prepared in tap water with an initial COD of 1280 mg/L. The working electrode Ti/$CoO_x$–$RuO_2$–$SnO_2$–$Sb_2O_5$ as functional DSA was indigenously prepared in laboratory by thermal decomposition method [3, 5, 9] using a precursor mixed metal salt solution. This solution consisted of $RuCl_3 \cdot xH_2O$ (99.9%, Aldrich), $SbCl_3$ (98.5%, CDH), $SnCl_4 \cdot 5H_2O$ (98% Aldrich) and $CoCl_2 \cdot 6H_2O$ (98% Aldrich) in iso-propanol (99.8% CDH, AR grade) and hydrochloric acid (37%, CDH). A metal molar ratio of Ru(15)/Co(15)/Sb(10)/Sn(60) was used. The precursor solution was then applied for about 10–12 coats on a pretreated Ti substrate (75 mm × 50 mm × 3 mm) using brush method to attain a mixed metal oxide catalytic loading of about 2–3 mg/cm$^2$ over the substrate. The sequential steps involved in electrode fabrication by thermal decomposition method using brush technique are illustrated in Fig. 2. The effective wetted surface area of the working electrode was ∼ 65 cm$^2$. Sulfuric acid was used for pH adjustment. NaCl, KBr and $Na_2SO_4$ were used as supporting electrolytes for electrolysis.

## Reactor Configuration and Operation Methodology

As shown in Fig. 3, an undivided cell with 1 L working reaction volume was used to conduct batch experiments at room temperature. The anode (Ti/$CoO_x$–$RuO_2$–$SnO_2$–$Sb_2O_5$) and cathode (stainless steel plate grade 304) each of dimension 75 mm × 50 mm × 3 mm were placed parallel

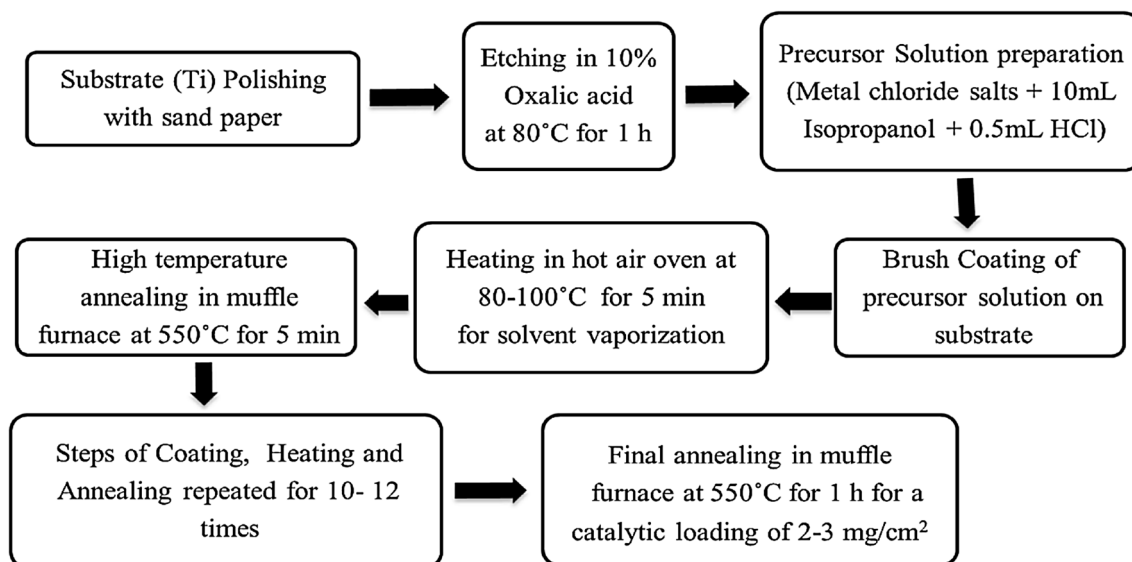J. Inst. Eng. India Ser. A (June 2019) 100(2):299–310

301



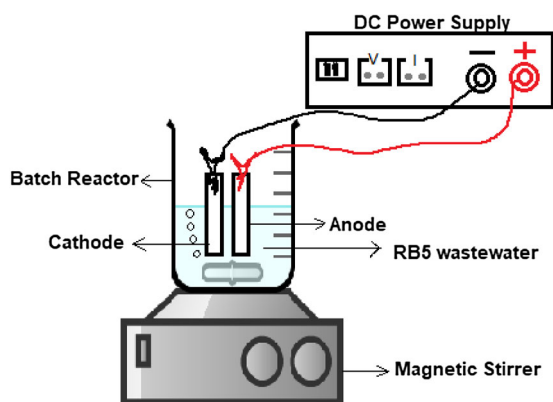Fig. 2 Stepwise electrode fabrication by thermal decomposition method using brush technique



Fig. 3 Experimental setup for electrooxidation

to each other with an interelectrode gap of 8 mm. These electrodes were dipped in 1000 ppm RB 5 solution. NaCl, KBr and $Na_2SO_4$ were used individually as supporting electrolytes in the reaction mixture with similar electrolysis parameters like electrolyte concentration of 0.07 M, pH 3, current density of 50 mA/cm$^2$ and electrolysis duration of 2 h. The solution was constantly stirred at $\sim$ 210 rpm with a magnetic stirrer in order to maintain uniform concentration of the reaction mixture. A DC power supply (Aplab India, LD-3205) with current–voltage monitor was used as a source of electric power for experimentation.

For each supporting electrolyte tested, treated effluent samples with a sample volume of 15 mL each were drawn every 10 min up to 60 min followed by sampling at 90 min and 120 min to assess reduction in pollution load in terms of COD, TOC and color intensity. pH change was also observed for each run during electrolysis. COD was determined using standard dichromate closed reflux

method (APHA standard 5220 C and D) using COD reactor supplied by Hach DRB200, USA. TOC was determined using TOC analyzer model (TOC-VCSH, Shimadzu, Japan).

## Results and Discussion

### Electrode Characterizations

SEM–EDAX Analysis

Scanning electron microscopy (SEM) characterization is used for high resolution imaging of surface microstructure of desired specimens using a focussed electron beam. Energy-dispersive X-ray spectroscopy (EDAX) in combination with SEM is used to provide identification of elements and information on their quantitative composition over selected imaged area of the specimen. During EDAX analysis, interactions occur between the specimen surface and the electromagnetic radiation in terms of X-rays emitted from the surface, which help in assessing the type and concentration of atoms of specific elements present. In case of electrode thin films, such information can be related to the effective surface area of the electrode and availability of catalytic active sites.

The oxide film surface morphology and composition of as-prepared $Ti/CoO_x–RuO_2–SnO_2–Sb_2O_5$ electrode was observed by using scanning electron microscopy (SEM, LEO 440 i). Figure 4 shows SEM micrograph of the electrode. The film showed a homogeneous morphology with a "cracked-clay" structure, which is typical of oxide films prepared by thermal decomposition method. This
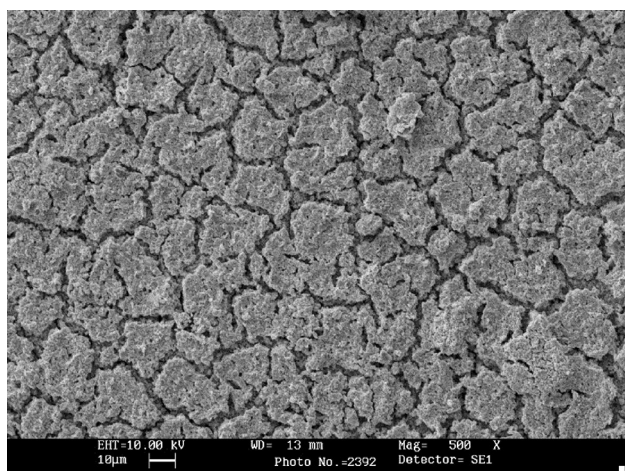
**Fig. 4** SEM micrograph of Ti/CoO$_x$–RuO$_2$–SnO$_2$–Sb$_2$O$_5$ electrode

type of structure offers high surface area to the electrode leading to more active sites and hence high catalytic activity [20, 21]. The elemental composition of as-prepared Ti/CoO$_x$–RuO$_2$–SnO$_2$–Sb$_2$O$_5$ electrode was analyzed using EDAX coupled with SEM (EDAX, SEM–EDAX LEO 440 i) as shown in Table 1. As seen from the table, the experimental composition of Sn is less compared to the nominal one because in thermal decomposition process, SnCl$_4$ volatilizes rapidly which leads to Sn loss of about 40–80% [22]. Figure 5 shows EDAX spectrum of a selected imaged area of the electrode clearly indicating the presence of characteristic elemental peaks of Co, Ru, Sn and Sb.

**Table 1** Quantitative analysis of metal concentration in Ti/CoO$_x$–RuO$_2$–SnO$_2$–Sb$_2$O$_5$ by EDAX

| Metal | Co | Ru | Sn | Sb |
|---|---|---|---|---|
| Nominal composition (wt%) | 15 | 15 | 60 | 10 |
| Experimental composition (wt%) | 27.05 | 26.15 | 17.22 | 29.58 |
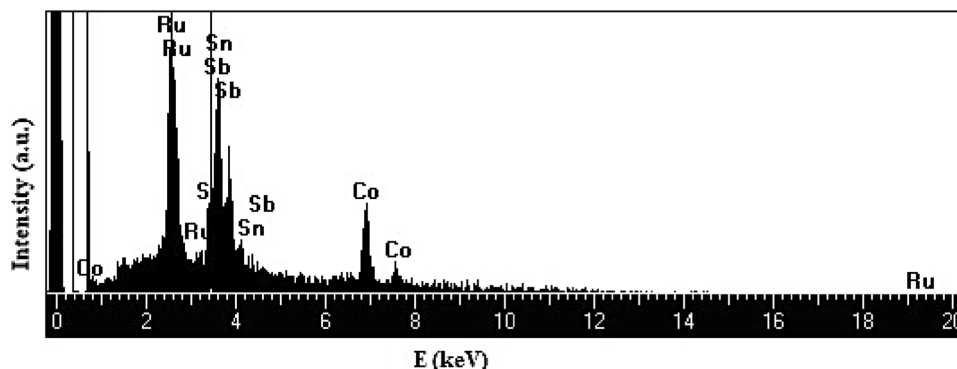
## XRD Analysis

X-Ray diffraction (XRD) is an important nondestructive technique for identifying phases of specimen and primarily works at atomic or molecular scale. The interference of monochromatic X-ray beam diffracted at specific angles from individual set of lattice planes in a specimen generates X-ray diffraction peaks, whose intensities are determined from the atomic distribution within the lattice. These X-ray diffraction patterns are matched with the standard Joint Committee on Powder Diffraction Standards (JCPDS) information to identify specific phases of the specimen.

In the present work, XRD was used to identify the phases of the mixed oxide film deposited over the anode. The crystal structure of as-prepared Ti/CoO$_x$–RuO$_2$–SnO$_2$–Sb$_2$O$_5$ electrode was investigated by X-ray diffractometer (XRD, Bruker D8 Advance) with Cu K$\alpha$ radiation ($\lambda = 1.5405$ Å) recorded with a step of 0.05° for $2\theta$ between 10 and 90°. Figure 6 shows XRD pattern of electrode. The characteristic peaks in XRD pattern were confirmed by the standard diffraction peaks. The peaks located at $2\theta = 19.02°$, 31.5°, 45.58°, 51.48° and 58.88° corresponded to cubic Co$_3$O$_4$ (JCPDS, No. 74-1656) [23]. The peaks located at $2\theta = 28.01°$, 35.05°, 39.55°, 54.16°, 66.02°, 70.39° and 77.02° corresponded to rutile RuO$_2$ (JCPDS, No. 40-1290) [21]. The peaks located at $2\theta = 39.55°$, 51.48°, 62.25° and 68.24° corresponded to Sb$_2$O$_5$ (JCPDS, No. 33-0110) [24]. The peaks located at $2\theta = 26.61°$, 33.89°, 61.86° and 66.02° corresponded to rutile SnO$_2$ (JCPDS, No. 41-1445) [21]. Thus, constituent metal peaks were clearly visible in EDAX spectrum whereas constituent metal oxide phases were detected with XRD analysis.

## Supporting Electrolytes and Electrochemical Oxidation Mechanisms

In direct anodic oxidation, adsorption of pollutants occurs at the anode surface followed by their degradation by anodic electron transfer reaction. In indirect oxidation,
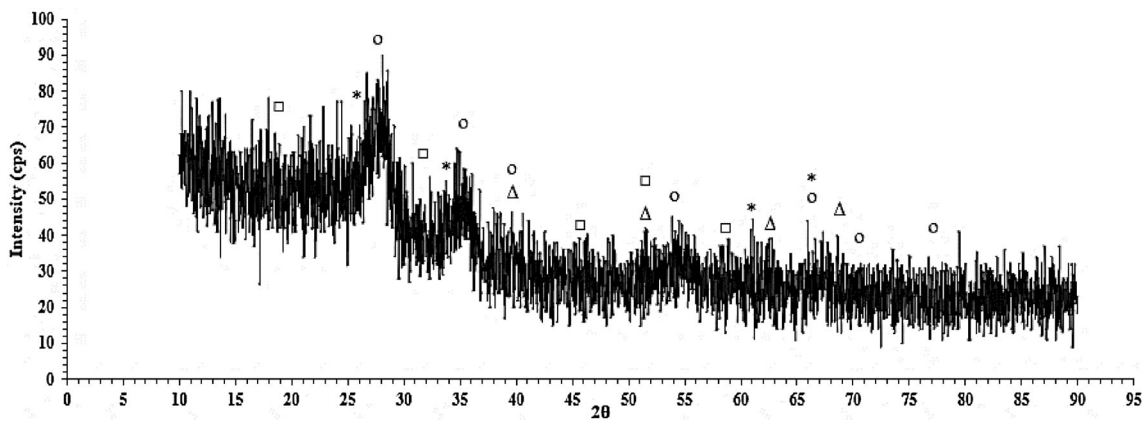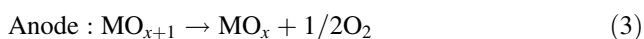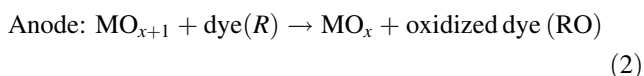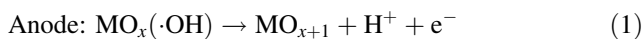
**Fig. 5** EDAX spectrum of Ti/CoO$_x$–RuO$_2$–SnO$_2$–Sb$_2$O$_5$ electrode

**Fig. 6** XRD pattern of Ti/CoO$_x$–RuO$_2$–SnO$_2$–Sb$_2$O$_5$ electrode indicating Co$_3$O$_4$ (□), RuO$_2$ (○), Sb$_2$O$_5$ (△), SnO$_2$ (*)

strong oxidants are electrochemically produced in situ which destroy the pollutants in the bulk solution. In the present case, when using mixed metal oxide anode (DSA) in indirect electrochemical oxidation of RB 5 dye in the presence of NaCl, KBr and Na$_2$SO$_4$ as supporting electrolytes, a major portion of oxidation is mediated by electrogenerated active chloro, bromo and sulfate species along with a possibility of direct oxidation at the anode surface. The proposed treatment mechanism for RB 5 degradation at Ti/CoO$_x$–RuO$_2$–SnO$_2$–Sb$_2$O$_5$ anode in the presence of each of these oxidant species is as follows [25, 26].
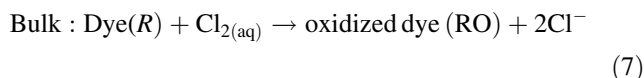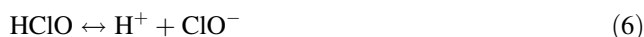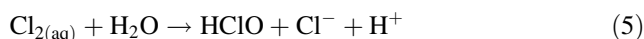
Direct Oxidation at the Anode Surface

The first step is of water dissociation resulting in the generation of hydroxyl (·OH) radicals during electrolysis. These ·OH radicals are chemisorbed at the mixed metal oxide anode represented by MO$_x$, and this strong interaction leads to the formation of a superoxide (MO$_{x+1}$) as per rxn (1). The chemically adsorbed oxygen in MO$_{x+1}$/MO$_x$ redox couple acts as an active site for selective oxidation of the dye (rxn (2)). The oxygen evolution reaction (OER) is a side reaction (rxn (3)) which competes with the dye oxidation reaction (rxn (2)).

$$\text{Anode: } MO_x(\cdot OH) \rightarrow MO_{x+1} + H^+ + e^- \tag{1}$$

$$\text{Anode: } MO_{x+1} + \text{dye}(R) \rightarrow MO_x + \text{oxidized dye}(RO) \tag{2}$$

$$\text{Anode : } MO_{x+1} \rightarrow MO_x + 1/2O_2 \tag{3}$$
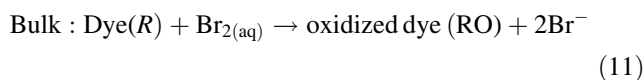
Indirect Oxidation by Chlorine Species

As per rxn (4), the oxidation of chloride (Cl$^-$) anion on the anode releases chlorine (Cl$_{2(aq)}$). As Cl$_{2(aq)}$ diffuses away from the anode, it is immediately hydrolyzed forming HClO and Cl$^-$ as shown by disproportionation rxn (5), with

the HClO being in acid–base equilibrium with hypochlorite anionic species indicated by rxn (6) with pKa = 7.55 [15]. Under acidic conditions, free chlorine is the dominant oxidizing agent, while under alkaline conditions hypochlorite, chloride ions and hydroxyl radicals are dominant species [4]. Further, dye is oxidized in the bulk medium via rxn (7) by active chlorine generated as per rxn (4) under acidic condition.

$$2Cl^- \rightarrow Cl_{2(aq)} + 2e^- \tag{4}$$

$$Cl_{2(aq)} + H_2O \rightarrow HClO + Cl^- + H^+ \tag{5}$$

$$HClO \leftrightarrow H^+ + ClO^- \tag{6}$$

$$\text{Bulk : Dye}(R) + Cl_{2(aq)} \rightarrow \text{oxidized dye (RO)} + 2Cl^- \tag{7}$$
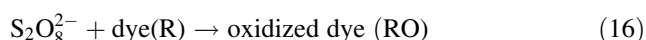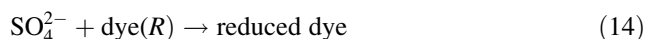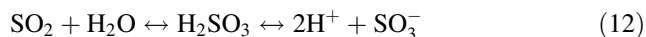
Indirect Oxidation by Bromine Species

Similarly, in case of KBr electrolyte, Br$_2$ formed at the anode undergoes reaction in the bulk solution to form HOBr or BrO$^-$. The production of active bromine species and their role in dye electrooxidation are represented by rxns (8)–(11).

$$2Br^- \rightarrow Br_{2(aq)} + 2e^- \tag{8}$$

$$Br_{2(aq)} + H_2O \rightarrow HOBr + Br^- + H^+ \tag{9}$$

$$HOBr \leftrightarrow H^+ + BrO^- \tag{10}$$

$$\text{Bulk : Dye}(R) + Br_{2(aq)} \rightarrow \text{oxidized dye (RO)} + 2Br^- \tag{11}$$

Indirect Oxidation/Reduction by Sulfate Species

Sulfate-based electrolytes are generally classified as inert and thus do not produce any reactive species during electrolysis. They may produce persulfate (S$_2$O$_8^{-2}$) under special conditions at inert electrodes like boron-doped diamond (BDD) [18]. The presence of Na$_2$SO$_4$ and other

304

J. Inst. Eng. India Ser. A (June 2019) 100(2):299–310

sulfate-containing electrolytes leads to the formation of $SO_2$ in acidic media which serves as a moderate reductant [4, 27]. Rxns (12)–(14) represent reactions related to dye reduction by $SO_2$ in acidic media at mixed metal oxide electrode (active anode). Rxns (15) and (16) show the dye oxidation reactions occurring at inert anodes (BDD) in presence of sulfate-based electrolytes.

$$SO_2 + H_2O \leftrightarrow H_2SO_3 \leftrightarrow 2H^+ + SO_3^- \qquad (12)$$

$$SO_3^- + [O] \rightarrow SO_4^{2-} \qquad (13)$$

$$SO_4^{2-} + \text{dye}(R) \rightarrow \text{reduced dye} \qquad (14)$$

$$2SO_4^{2-} \rightarrow S_2O_8^{2-} + 2e^- \qquad (15)$$

$$S_2O_8^{2-} + \text{dye}(R) \rightarrow \text{oxidized dye (RO)} \qquad (16)$$

Reaction at the Cathode

Rxn (17) represents the reaction taking place at the cathode to generate $H_2$ gas and $OH^-$.

$$\text{Cathode}: 2H_2O_{(aq)} + 2e^- \rightarrow H_{2(g)} + 2OH^-_{(aq)} \qquad (17)$$
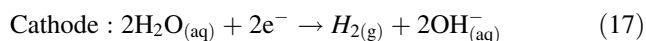
Effect of Supporting Electrolyte on COD and TOC Decay

The degradation process of the dye wastewater is monitored from the abatement of its COD and TOC. The percentages of COD and TOC decays are estimated from Eqs. (18) and (19), respectively [14].

$$\text{COD decay } (\%) = \frac{\Delta COD}{COD_0} \times 100 \qquad (18)$$

$$\text{TOC decay } (\%) = \frac{\Delta TOC}{TOC_0} \times 100 \qquad (19)$$

where $\Delta COD$ and $\Delta TOC$ are the corresponding removals in COD and TOC in mg/L at electrolysis time $t$; $COD_0$ and $TOC_0$ are their initial values before treatment. Figures 7 and 8 show the percentage COD and TOC decay, respectively, as a function of time for individual electrolytes used. It is clear that COD removals were 40.2, 31.2 and 13.0% and TOC removals were 26.5, 22.5 and 7.7%, respectively, with NaCl, KBr and $Na_2SO_4$ electrolytes at the end of 2-h electrolysis.

In acidic conditions, $Cl_2$ and HClO are the main oxidative species when NaCl is used [13, 28]. Similar is the case with KBr, while the use of $Na_2SO_4$ generates relatively inert species $SO_2$ [18]. The standard potentials of $Cl_2/Cl^-$, $Br_2/Br^-$ and $SO_4^{2-}/SO_2$ are + 1.36 V, + 1.08 V and + 0.17 V, respectively, and that of $ClO^-$ and $BrO^-$ are + 0.89 V and + 0.74 V, respectively, which makes chlorine a powerful oxidizing agent over bromine and sulfate due to its strong attraction for electrons [13, 29]. Thus the "active chlorine" species imparts high oxidation rate in terms of COD abatement and mineralization rate in terms
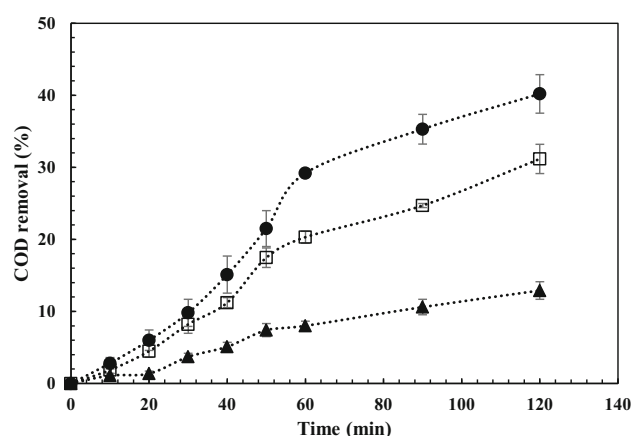


**Fig. 7** Removal of COD with electrolysis time in 0.07 M NaCl (●), 0.07 M KBr (□) and 0.07 M $Na_2SO_4$ (▲)
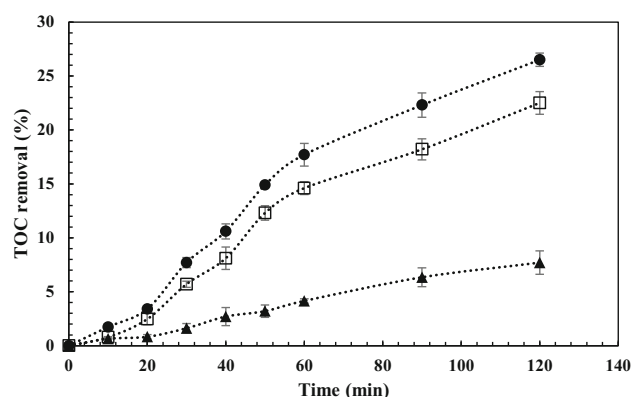


**Fig. 8** Removal of TOC with electrolysis time in 0.07 M NaCl (●), 0.07 M KBr (□) and 0.07 M $Na_2SO_4$ (▲)

of TOC abatement of dye effluent compared to active bromine and inert sulfate species in acidic medium under indirect electrochemical oxidation mechanism.

Effect of Supporting Electrolyte on Color Removal

Color intensity was measured at a maximum absorbance wavelength ($\lambda_{max}$) = 597 for RB 5 using UV/Vis spectrophotometer model (1800, Shimadzu, Japan). Color removal was calculated by using the following Eq. (20) [14].

$$\text{Color removal } (\%) = \frac{ABS_0 - ABS_t}{ABS_0} \times 100 \qquad (20)$$

where $ABS_0$ and $ABS_t$ are absorbances before and after electrolysis time $t$, respectively, at the maximum visible wavelength ($\lambda_{max}$) of wastewater. Figure 9 shows the percentage of color removal with respect to time for investigated electrolytes. Figure 10 shows UV–Vis spectra of untreated and electrochemically treated dye effluent for all electrolytes. From Fig. 8, it is seen that the color removal
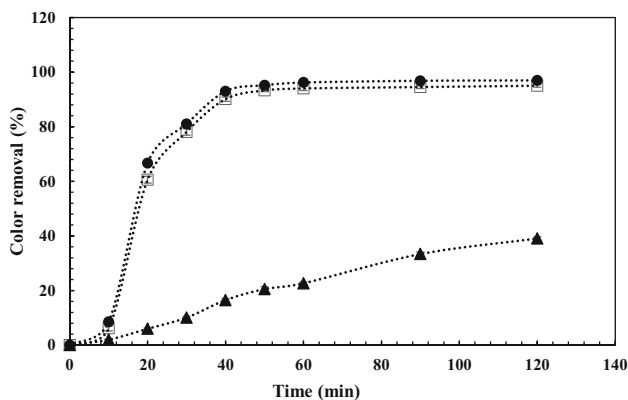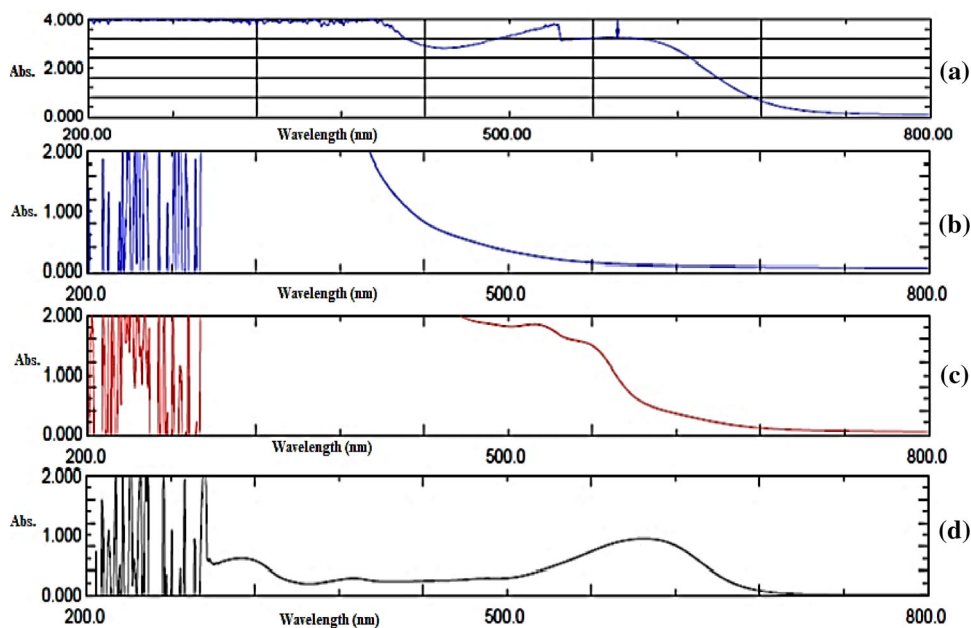
**Fig. 9** Removal of color with electrolysis time in 0.07 M NaCl (●), 0.07 M KBr (□) and 0.07 M Na$_2$SO$_4$ (▲)

was 97, 95 and 39%, respectively, with NaCl, KBr and Na$_2$SO$_4$ at the end of 2-h electrolysis. Maximum decolorization was achieved within almost 40 min in the presence of NaCl and KBr while that for Na$_2$SO$_4$ was found to be least as acidic conditions favored decolorization in NaCl and KBr electrolytes [3].

It is observed that color reduction is due to the cleavage of chromophore groups or azo bond in the dye molecule which further results in decolored intermediates in the bulk solution [3, 10]. This leads to decolorization within a short time period than their respective COD decays as oxidation of aromatic rings takes relatively longer times. Also, COD removals were observed to be less compared to decolorization extents due to the formation of low molecular weight aliphatic compounds which resist attack by electroactive oxidant species [10]. The spectra in Fig. 10 indicate that almost complete disappearance of the signature peak of RB 5

dye at $\lambda_{max}$ = 597 was observed for NaCl and KBr which meant a complete effluent decolorization.

**Supporting Electrolyte and pH Variation**

It has been reported that acidic pH favors faster oxidation of organics when mediated by electrogenerated active species [16]. Particularly, active chlorine species present higher oxidation ability and thus impart higher COD conversion for both real and synthetic effluents at acidic pH [4, 17]. Thus, an initial pH 3 was taken for all experiments in the present work. Figure 11 shows pH change with respect to time for investigated electrolytes.

It is clear that within almost 40 min, the initial acidic pH changed to near neutral which then remained constant. This may be due to the reaction between OH$^-$ and CO$_2$ (degradation product), thereby generating bicarbonate buffer during electrooxidation of organics [4, 18]. In case of Na$_2$SO$_4$, pH change was not prominent which may be due to low TOC conversion resulting in very low CO$_2$ formation. Thus, the use of NaCl and KBr electrolytes eliminates the need of neutralizing the treated effluent for further reuse or discharge.

**Supporting Electrolyte and Average Current Efficiency (ACE)**

Current efficiency, also known as electrical yield, is referred to as the ratio of electrical charge actually used to oxidize the organic matter to the total consumed electrical charge. At a given electrolysis time $t$, the average current efficiency (ACE) [10] can be determined as per Eq. (21)

**Fig. 10** UV–Vis spectra of untreated and treated dye effluent during electrochemical oxidation: **a** untreated effluent, **b** treated with 0.07 M NaCl after 2-h electrolysis, **c** treated with 0.07 M KBr after 2-h electrolysis and **d** treated with 0.07 M Na$_2$SO$_4$ after 2-h electrolysis
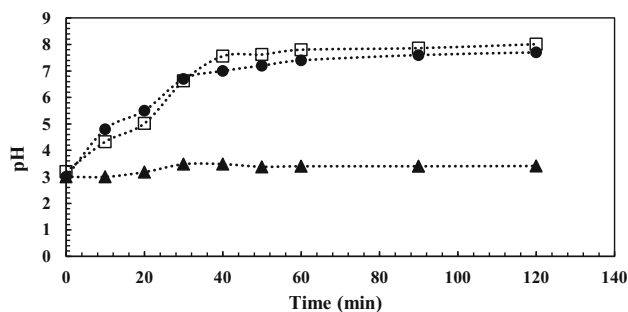
**Fig. 11** pH change with electrolysis time in 0.07 M NaCl (●), 0.07 M KBr (□) and 0.07 M Na$_2$SO$_4$ (▲)

$$ACE\,(\%) = \frac{(COD_0 - COD_t)\,F\,V_s}{8It} \times 100 \tag{21}$$

where $COD_0$ and $COD_t$ are the COD values (mg/L) at initial time and at given electrolysis time $t$, respectively, $F$ is the Faraday constant (96,487 C/mol), $V_s$ is the solution volume (L), $I$ is the applied current (A), 8 is the oxygen equivalent mass (g/eq) and $t$ is the treatment time (h). Figure 12 highlights the ACE determined for different electrolytes tested. As expected, the ACE dropped in sequence: NaCl (53.9%) > KBr (41.8%) > Na$_2$SO$_4$ (17.3%) at the end of 2-h electrolysis. Based on this, it can be said that the degradation mechanism in the presence of NaCl was controlled by charge transfer. This also means that the electrode surface becomes highly polarized and produces a greater concentration of "active chlorine" which finally results in a greater degradation of the dye and intermediates [3]. Lower ACE values as in case of Na$_2$SO$_4$ also imply larger fraction of applied current used for parallel undesired oxygen evolution side reaction (OER) which serves as a limiting step in organics oxidation [5].

Supporting Electrolyte and Energy Consumption (EC)

Energy consumption (kWh/kg COD and kWh/kg TOC) [10, 11] helps to assess commercial feasibility of electrochemical treatment. It is calculated by Eqs. (22) and (23)
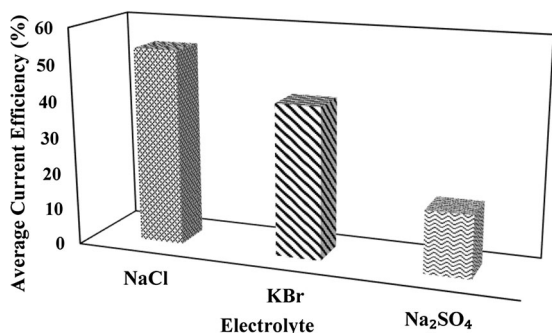
$$EC(\text{kWh/kg COD}) = \frac{E_{cell}It}{3.6(COD_0 - COD_t)V_s} \tag{22}$$

$$EC\,(\text{kWh/kg TOC}) = \frac{E_{cell}It}{3.6(TOC_0 - TOC_t)V_s} \tag{23}$$

where $COD_0$ and $COD_t$ are the COD values (mg/L) at initial time and at given electrolysis time $t$, respectively, $TOC_0$ and $TOC_t$ are the TOC values (mg/L) at initial time and at given electrolysis time $t$, respectively, $E_{cell}$ is the average voltage applied (V), $t$ is the treatment time (h) and $V_s$ is the solution volume (L). Figure 13 shows EC estimated based on COD and TOC mass for different electrolytes tested. It is seen that EC based on COD were 11.1, 14.3 and 34.5 kWh/kg COD and EC based on TOC were 85.7, 101.9 and 302.9 kWh/kg TOC with NaCl, KBr and Na$_2$SO$_4$ electrolytes, respectively, at the end of 2-h electrolysis. This showed least energy consumption resulting in low process cost in case of NaCl and hence NaCl is clearly preferred to be used over KBr and Na$_2$SO$_4$.

Kinetics of COD and Dye Removal

In indirect oxidation process, the COD removal rate is proportional to the concentration of pollutant and to the electrogenerated active oxidant species. These oxidant species oxidize the pollutant and get reduced. This process gets repeated in a catalytic manner which allows the oxidant species concentration to remain constant and thus results in a psuedo-first-order kinetic equation given by Eq. (24) [13, 18].

$$\frac{-d[COD]}{dt} = k\,[COD] \tag{24}$$

The log plot of the COD concentration curve given by Eq. (25) represents the plot of the rate expression whose slope gives the value of rate constant $k$ (time$^{-1}$)

$$\log \frac{[COD]}{[COD]_0} = -k\,t \tag{25}$$



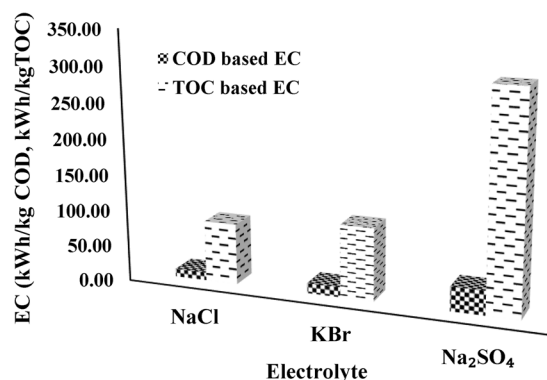**Fig. 12** ACE (%) in different electrolytes



**Fig. 13** Energy consumption in different electrolytes

Figure 14 shows the plot of dimensionless COD against electrolysis time for all the three electrolytes. From Fig. 14, the kinetic constant ($k$) values evaluated using Eq. (25) were found to be 0.0046, 0.0033 and 0.0013 min$^{-1}$ for NaCl, KBr and Na$_2$SO$_4$, respectively, which implied fastest pollutant degradation rate with respect to NaCl owing to highest oxidation power of active chlorine species. Figure 15 shows the normalized dye concentration ($C/C_o$) plot against electrolysis time for all the three electrolytes where $C_o$ is initial dye concentration and $C$ is dye concentration at corresponding electrolysis time. From Fig. 15, it is evident that dye concentration diminishes rapidly to almost complete dye elimination in case of NaCl and KBr at the end of electrolysis while for Na$_2$SO$_4$, there is a slow decrease in dye concentration with relatively lesser extent of dye elimination.

Fate of Electrolytes After Electrochemical Oxidation

The reduction in concentration of individual electrolyte during electrolysis was investigated using an indirect method of measuring reaction mixture conductivity using
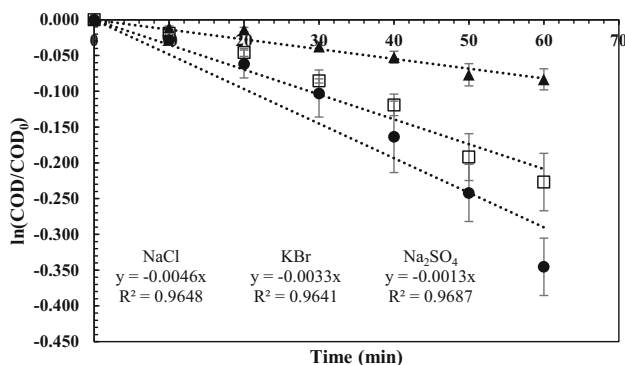


**Fig. 14** Plot of COD/COD$_o$ versus electrolysis time for NaCl (●), KBr (□) and Na$_2$SO$_4$ (▲)
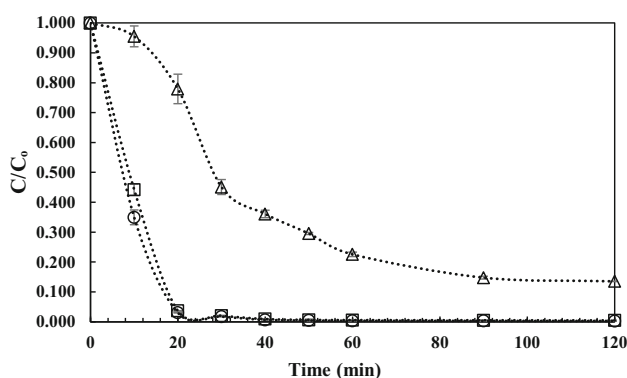


**Fig. 15** Plot of $C/C_o$ versus electrolysis time for NaCl (○), KBr (□) and Na$_2$SO$_4$ (△)

digital conductivity meter (EQ-664A, Equip-Tronics) at reaction times of $t = 0$ min, 60 min and 120 min and correlating it with the electrolyte concentration. Figure 16 shows the normalized electrolyte concentration ($C_s/C_{so}$) plot against time. From this plot, the decrease in conductivity and hence concentration for NaCl and KBr is more pronounced compared to Na$_2$SO$_4$ indicating the discharge of chlorine (Cl$_2$) and bromine (Br$_2$) at the anode [30]. At the end of 2-h electrolysis, concentrations were found to drop from 0.07 M to 0.0589 M for NaCl, 0.07 M to 0.0593 M for KBr and 0.07 M to 0.0620 M for Na$_2$SO$_4$.

### Degradation Products

Liquid chromatography–mass spectrometry (LC–MS) is an analytical method integrated with chromatographic separation to detect mass spectrum of complex liquid-phase mixtures with high sensitivity and specificity under positive and negative operational modes using electrospray ionization (ESI). During LC–MS analysis, sample liquid mixture is pumped through a metal capillary at $\sim$ 5 kV to form a fine mist or spray of charged droplets at the capillary tip. These ionized or charged analyte molecules of the liquid mixture are then transferred to the mass spectrometer where the ions and fragment ions produced are analyzed based on their mass-to-charge ratio ($m/z$) by the use of ion source and subsequent ion optics. Consequently, mass spectrum (ES+/ES−) is generated by plotting ion signal versus $m/z$ ratio which is further used to ascertain the mass of specific molecules and fragments with elucidation of their chemical structures.

In the present study, LC–MS technique was employed to analyze the mass fragments of RB 5 dye effluent before and after 60 min electrolysis in presence of NaCl electrolyte. Figure 17a shows the ES− mass spectrum of the dye solution before electrolysis, and Fig. 17b shows the ES− mass spectrum of the degraded dye. Tables 2 and 3 show the identified characteristic $m/z$ peaks of molecular and product ions of RB 5 dye effluent before and after electrolysis which have been confirmed with the literature ($\geq$ 95% match) [31–33]. As evident from Fig. 17b, majority of earlier peaks of spectrum in Fig. 17a have disappeared due to decomposition of dye solution into low molecular weight compounds. After extended RB 5 electrolysis in chloride medium, formation and proposed structures of different chlorinated and highly polar organic and inorganic products are reported with further need for undertaking toxicity studies. Nuclear magnetic resonance (NMR)-based techniques are required to identify all possible degradation products including structural isomers with increased precision [33].

**Fig. 16** Plot of $C_s/C_{so}$ versus electrolysis time for NaCl (●), KBr (□) and Na₂SO₄ (▲)
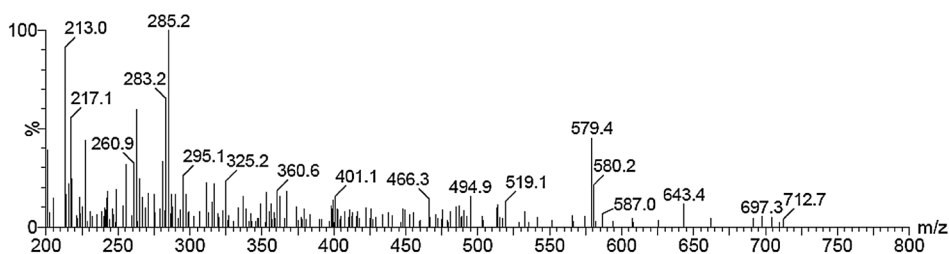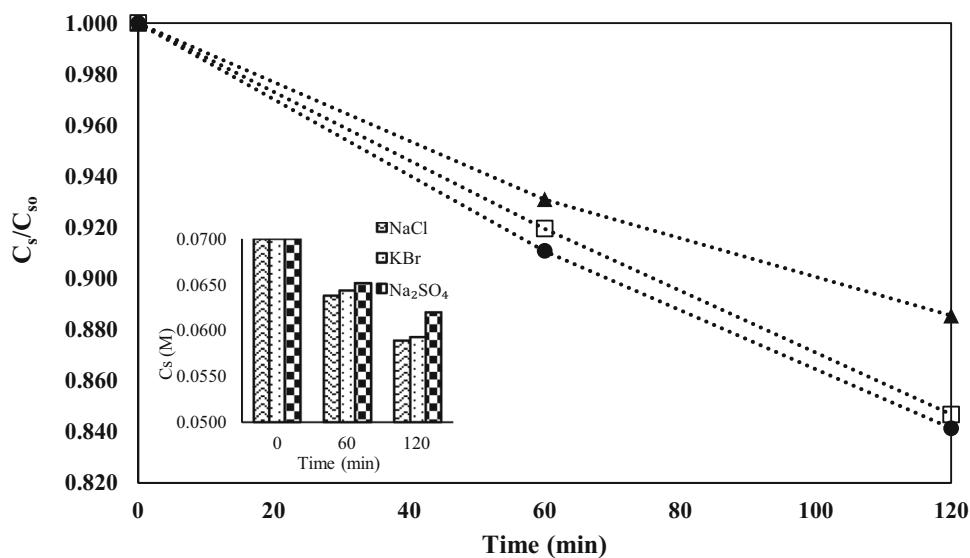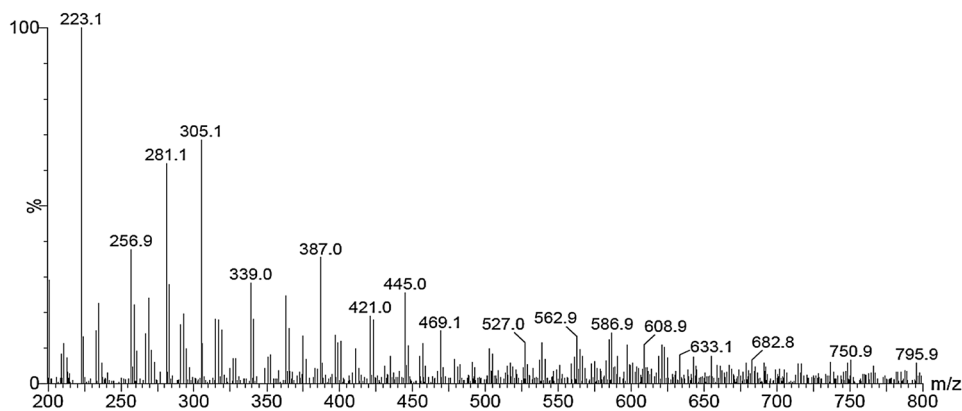




**Fig. 17 a** (ES−) Mass spectrum of RB 5 dye effluent before electrolysis. **b** (ES−) Mass spectrum of RB 5 dye effluent after 60-min electrolysis

## Conclusions

The indirect electrochemical degradation of simulated wastewater containing high concentration of RB 5 has been investigated in NaCl, KBr and Na₂SO₄ as supporting electrolytes under similar operating conditions using Ti/CoO$_x$–RuO₂–SnO₂–Sb₂O₅ electrode. The results of this study revealed the following:

1.  The highest electrocatalytic performance was achieved in terms of reduction in COD, TOC and color intensity under acidic pH in the presence of NaCl compared to KBr and Na₂SO₄ since chloride acts as a high oxidation power electrogenerated active species compared to bromide and sulfate.
2.  Performance in NaCl electrolyte offered highest average current efficiency, almost three times more than

**Table 2** $m/z$ for RB 5 effluent before electrolysis

| $m/z$ (experimental— Fig. 16a) | $m/z$ (matched with the literature) | Ions in MS |
|---|---|---|
| 466.3 | 461.458 | $[M–3H+Na]^{2-}$ |
| 360.6 | 361.501 | $[M–2H–SO_3]^{2-}$ |
| 401.1 | 401.483 | $[M–2H–H_2SO_4]^{2-}$ |
| 579.4 | 533.967 | $[M–3H+Na]^{2-}$ |
| 643.4 | 642.0 | $[M–H–2H_2SO_4–SO_2]^{-}$ |

**Table 3** $m/z$ for RB 5 effluent product ions after electrolysis

| $m/z$ (experimental— Fig. 16b) | Ions observed in first-order $m/z$-structure (matched with the literature) | Product ions in MS $m/z$-structure (matched with the literature) |
|---|---|---|
| 223.1 | $223 – [M–2H–SO_3+Na]^{-}$ | $224 – [M–H–H_2SO_4–C_2H_3]^{-}$ |
| | $238 – [M–2H–SO_2+Na]^{-}$ | $217 – [M–H–SO_2]^{-}$ |
| 281.1 | $280 – [M–H]^{-}$ | $284 – [M–H–SO_2]^{-}$ |
| | $281 – [M–H]^{-}$ | $263 – [M–H–H_2O]^{-}$ |
| | | $268 – [M–H–SO_3]^{-}$ |
| | | $253 – [M–H–C_2H_3]^{-}$ |
| 339 | $348 – [M–H]^{-}$ | $331 – [M–H–NH_3]^{-}$ |
| | $349 – [M–H]^{-}$ | $330 – [M–H–H_2O]^{-}$ |
| | | $331 – [M–H–H_2O]^{-}$ |
| | | $313 – [M–H–HCl]^{-}$ |
| 387 | $370 – [M–2H+Na]^{-}$ | |
| | $371 – [M–2H+Na]^{-}$ | |
| 421 | $435.990 – [M–H]^{-}$ | $407.996 – [M–H–CO_2]^{-}$ |

$Na_2SO_4$ and least energy consumption compared to KBr and $Na_2SO_4$ owing to charge transfer controlled degradation mechanism and suppression of limiting side OER.

3. There is no need to add electrolyte separately as chloride is normally present in high concentration in dye effluents which also reduces the cost factor.

4. With NaCl and KBr, pH changed from acidic to neutral/alkaline at the end of electrolysis which eliminates the need of neutralizing the treated effluent further. In case of $Na_2SO_4$, pH remained almost constant due to low TOC decay resulting in very low $CO_2$ generation.

5. COD removal rate followed pseudo-first-order kinetics with the fastest degradation occurring in NaCl as evident from the rate constant $k$.

6. In presence of chloride medium, dye solution was degraded into low molecular weight fragments as observed from the LC–MS study conducted for RB 5 effluent before and after electrolysis.

Above results make NaCl a preferred electrolyte over KBr and $Na_2SO_4$ under given conditions for electrocatalytic degradation of highly concentrated effluents from dyes industries in general and for RB 5 in particular.

## References

1. N. Mohan, N. Balasubramanian, C.A. Basha, Electrochemical oxidation of textile wastewater and its reuse. J. Hazard. Mater. **147**(1–2), 644–651 (2007)
2. M. Panizza, G. Cerisola, Removal of colour and COD from wastewater containing acid blue 22 by electrochemical oxidation. J. Hazard. Mater. **153**(1–2), 83–88 (2008)
3. A.I. del Rio, M.J. Benimeli, J. Molina, J. Bonastre, F. Cases, Electrochemical treatment of C.I. reactive black 5 solutions on stabilized doped Ti/SnO₂ electrodes. Int. J. Electrochem. Sci. **7**(12), 13074–13092 (2012)
4. E. Chatzisymeon, N.P. Xekoukoulotakis, A. Coz, N. Kalogerakis, D. Mantzavinos, Electrochemical treatment of textile dyes and dyehouse effluents. J. Hazard. Mater. **137**(2), 998–1007 (2006)
5. R.G. Da Silva, S.A. Neto, A.R. De Andrade, Electrochemical degradation of reactive dyes at different DSA® compositions. J. Braz. Chem. Soc. **22**(1), 126–133 (2011)
6. A.J. Mendez-Martinez, M.M. Davila-Jimenez, O. Ornelas-Davila, M.P. Elizalde-Gonzalez, U. Arroyo-Abad, I. Sires, E. Brillas, Electrochemical reduction and oxidation pathways for Reactive Black 5 dye using nickel electrodes in divided and undivided cells. Electrochim. Acta **59**, 140–149 (2012)
7. E. Brillas, C.A. Martínez-Huitle, Decontamination of wastewaters containing synthetic organic dyes by electrochemical methods. An updated review. Appl. Catal. B Environ. **166–167**, 603–643 (2015)
8. H. Jalife-Jacobo, R. Feria-Reyes, O. Serrano-Torres, S. Gutierrez-Granados, J.M. Peralta-Hernandez, Diazo dye Congo Red degradation using a Boron-doped diamond anode: an experimental study on the effect of supporting electrolytes. J. Hazard. Mater. **319**, 78–83 (2016)
9. S. Aquino Neto, A.R. de Andrade, Electrooxidation of glyphosate herbicide at different DSA® compositions: pH, concentration and supporting electrolyte effect. Electrochim. Acta **54**(7), 2039–2045 (2009)
10. M.S. Morsi, A.A. Al-Sarawy, W.A.S. El-Dein, Electrochemical degradation of some organic dyes by electrochemical oxidation on a Pb/PbO₂ electrode. Desalin. Water Treat. **26**(1–3), 301–308 (2011)
11. A. Uranga-Flores, C. De La Rosa-Juarez, S. Gutierrez-Granados, D.C. De Moura, C.A. Martinez-Huitle, J.M. Peralta Hernández, Electrochemical promotion of strong oxidants to degrade Acid Red 211: effect of supporting electrolytes. J. Electroanal. Chem. **738**, 84–91 (2015)
12. F.L. Guzman-Duque, R.E. Palma-Goyes, I. Gonzalez, G. Penuela, R.A. Torres-Palma, Relationship between anode material, supporting electrolyte and current density during electrochemical degradation of organic compounds in water. J. Hazard. Mater. **278**, 221–226 (2014)

310

J. Inst. Eng. India Ser. A (June 2019) 100(2):299–310

13. D. Rajkumar, K. Palanivelu, N. Mohan, Electrochemical degradation of resorcinol using mixed oxide coated titanium electrode for wastewater treatment—a kinetic study. Indian J. Chem. Technol. **10**, 396–401 (2003)

14. C.A. Martinez-Huitle, E. Brillas, Decontamination of wastewaters containing synthetic organic dyes by electrochemical methods: a general review. Appl. Catal. B Environ. **87**(3–4), 105–145 (2009)

15. W. Wu, Z.H. Huang, T.T. Lim, Recent development of mixed metal oxide anodes for electrochemical oxidation of organic pollutants in water. Appl. Catal. A Gen. **480**, 58–78 (2014)

16. S. Garcia-Segura, J.D. Ocon, M.N. Chong, Electrochemical oxidation remediation of real wastewater effluents—a review. Process Saf. Environ. Prot. **113**, 48–67 (2018)

17. F.C. Moreira, R.A.R. Boaventura, E. Brillas, V.J.P. Vilar, Electrochemical advanced oxidation processes: a review on their application to synthetic and real wastewaters. Appl. Catal. B Environ. **202**, 217–261 (2017)

18. D. Rajkumar, J.G. Kim, K.K. Kim, A study on electrochemical oxidation of catechol in chloride medium for wastewater treatment application. Environ. Eng. Res. **9**(6), 279–287 (2004)

19. V.M. Vasconcelos, F.L. Ribeiro, F.L. Migliorini, S.A. Alves, J.R. Steter, M.R. Baldan, N.G. Ferreira, M.R.V. Lanza, Electrochemical removal of Reactive Black 5 azo dye using non-commercial boron-doped diamond film anodes. Electrochim. Acta **178**, 484–493 (2015)

20. C.R. Costa, C.M.R. Botta, E.L.G. Espindola, P. Olivi, Electrochemical treatment of tannery wastewater using DSA® electrodes. J. Hazard. Mater. **153**, 616–627 (2008)

21. H. Bai, P. He, J. Chen, K. Liu, H. Lei, X. Zhang, F. Dong, H. Li, Electrocatalytic degradation of bromocresol green wastewater on $Ti/SnO_2–RuO_2$ electrode. Water Sci. Technol. **77**(7), 1–8 (2016)

22. S. Chen, Y. Zheng, S. Wang, X. Chen, $Ti/RuO_2–Sb_2O_5–SnO_2$ electrodes for chlorine evolution from seawater. J. Chem. Eng. **172**, 47–51 (2011)

23. Y. Zhang, C. Meng, Facile fabrication of $Fe_3O_4$ and $Co_3O_4$ microspheres and their influence on the thermal decomposition of ammonium perchlorate. J. Alloys Compd. **674**, 259–265 (2016)

24. A.K. Srivastava, B. Yadav, Humidity sensing properties of $TiO_2–Sb_2O_5$ nanocomposite. Mater. Sci. **28**, 491–502 (2010)

25. A.N. Subba Rao, V.T. Venkatarangaiah, Metal oxide-coated anodes in wastewater treatment. Environ. Sci. Pollut. Res. **21**(5), 3197–3217 (2014)

26. D. Rajkumar, J.G. Kim, Oxidation of various reactive dyes with in situ electro-generated active chlorine for textile dyeing industry wastewater treatment. J. Hazard. Mater. **136**(2), 203–212 (2006)

27. A.H. Gemeay, Kinetics and mechanism of the reduction of some azo-dyes by inorganic oxysulfur compounds. Dyes Pigments **54**(3), 201–212 (2002)

28. F.L. Souza, D.W. Miwa, M.A. Rodrigo, A.J. Motheo, Electrochemical degradation of dimethyl phthalate ester on a DSA® electrode. Braz. Chem. Soc. **25**(3), 492–501 (2014)

29. M. Sun, G.V. Lowry, K.B. Gregory, Selective oxidation of bromide in wastewater brines from hydraulic fracturing. Water Res. **47**(11), 3723–3731 (2013)

30. G. Bhaskar Raju, M. Thalamadai Karuppiah, S.S. Latha, D. Latha Priya, S. Parvathy, S. Prabhakar, Electrochemical pretreatment of textile effluents and effect of electrode materials on the removal of organics. Desalination **249**(1), 167–174 (2009)

31. M. Holcapek, K. Volna, D. Vanerkova, Effects of functional groups on the fragmentation of dyes in electrospray and atmospheric pressure chemical ionization mass spectra. Dyes Pigments **75**(1), 156–165 (2007)

32. D. Vanerkova, A. Sakalis, M. Holcapek, P. Jandera, A. Voulgaropoulos, Analysis of electrochemical degradation products of sulphonated azo dyes using high-performance liquid chromatography/tandem mass spectrometry. Rapid Commun. Mass Spectrom. **20**, 2807–2815 (2006)

33. D. Jager, D. Kupka, M. Vaclavikova, L. Ivanicova, G. Gallios, Degradation of Reactive Black 5 by electrochemical oxidation. Chemosphere **190**, 405–416 (2018)